NOTICE CONCERNING COPYRIGHT RESTRICTIONS

Geothermal Resources Council, TRANSACTIONS Vol. 5, October 1981

FAILURE STUDIES ON TEXAS GULF COAST GEOPRESSURED-GEOTHERMAL SANDSTONES AND SHALES

P. N. Jogi, B. C. Llewellyn and K. E. Gray

Center for Earth Sciences and Engineering
University of Texas at Austin

Abstract

Triaxial compression tests were run at room temperature to determine failure characteristics of rocks extracted from the geopressured-geothermal reservoir underlying Brazoria county. Effects of both confining & pore fluid pressure were considered. Like all other rocks, ultimate strength was found to increase with increase in effective confining pressure. Partial ductile behavior was observed at pressures above 5000 psi. In general rocks from this reservoir were found to be considerably weaker than corresponding well compacted sandstones.

Introduction

Geopressured reservoirs are deep sedimentary basins filled with sand, clay or shale and are generally under-compacted below the depths of 7000 to 25000'.[1] As a result, part of the overburden pressure is carried by the interstitial pore fluid. For controlled exploitation of such reservoirs, it is necessary to determine the reservoir behavior under various stress conditions. One of the studies which is of importance to both geologists and drilling engineers is the knowledge of the in-situ failure characteristics of such rock formations.

The studies reported herein were conducted on samples extracted (from depths 11000-16000') from two test wells drilled in Brazoria county, Texas. Geological studies of samples extracted from this reservoir reveal that major types of porosity encountered are microporosity and secondary dissolution porosity, the later being dominant.[2] The behavior of these rocks under triaxial conditions of stress is, therefore, expected to be somewhat different from those of well compacted rocks, like Berea sandstone, limestones, and dolomites, test results for which have been reported in the literature.[3,4] Experiments[3,4] also show that limestones and dolomites, which are also characterized by secondary porosity, show transition from brittle to ductile behavior at much lower effective confining pressures than those for sandstones which are formed by grain to grain contact.

Most studies in the past[3] were conducted to study the effects of confining pressure on rock strengths; pore pressure in these studies was maintained constant. Several investigators[4-7], however, recognized that since the state of stress in a rock is determined by effective stress, therefore, a better understanding of the mechanism of rock failure could be obtained by studying the effects of both confining and pore fluid pressure on rock strength. Such studies[5,6,7] showed that the effective stress theory was applicable and that the magnitudes of confining pressure and pore fluid pressure had no effect on rock strength as long as they were equal but mode of failure changed from brittle to ductile when the effective confining pressure increased.

In order to have a better understanding of the mechanism of failure in rock samples from the geopressured reservoir (depths 11000-16000'), tests were conducted to study the effects of both confining and pore pressure on rock strength at room temperature while maintaining a constant strain rate. The results from these tests are discussed in detail in the following sections.

Theoretical Considerations

The conclusions from the data of these tests are based on the assumption of Coulomb-Mohr friction hypothesis and the concept of effective stress. According to Coulomb-Mohr criterion, failure occurs when shearing stress exceeds the sum of cohesive strength, τ_0, and frictional resistance to slip along the failure plane and is given by

$$\tau = \tau_0 + \sigma_n \tan \phi \qquad (1)$$

where ϕ is the angle of friction and is related to coefficient of internal friction μ by

$$\mu = \tan \phi \qquad (2)$$

Effective normal and shear stresses σ_n and τ are given by

$$\sigma_n = \frac{\sigma_1+\sigma_3}{2} - \frac{\sigma_1-\sigma_3}{2} \operatorname{Cos} 2\theta$$
$$\tau = \frac{\sigma_1-\sigma_3}{2} \operatorname{Sin} 2\theta \qquad (3)$$

where θ = angle between the failure plane and the major principal axis.

The data from a series of triaxial tests were used to plot Mohr circles for each pair of effective stresses σ_1 and σ_3 on the sample (Fig. 3). The Mohr's envelope, which is a curve tangent to all these circles, is the locus of all points satisfying Eqn. (1). Fracture angle θ, angle of friction ϕ, and shear stress τ can be obtained from Mohr envelope as shown in Fig. (3). From this figure it is evident that

$$\theta = 45^0 + \frac{\phi}{2} \qquad (4)$$

Experimental Arrangement & Test Procedure

The experimental set up to study the strength characteristics of the rocks is shown in Fig. (1). The compression cell, designed for working pressures up to 15000 psi with an independent control for axial load, confining pressure and pore pressure is similar to the one used by Robinson.[5]

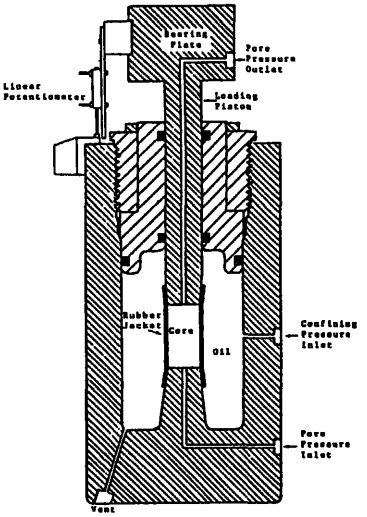

FIGURE 1 EXPERIMENTAL SET-UP

All tests were run on a 1" diameter x 2" long samples cut from cores extracted from 12 different depths (as indicated in Table I) representing a wide cross-section of the producing zones of the two wells. Four to six samples were cut from each core for each test.

Each sample, saturated with a 6% salt solution, was initially loaded hydrostatically to the desired confining and pore pressure by increasing the confining pressure, pore pressure and axial load simultaneously in steps of 500 psi. The desired confining pressure was determined by half the in-situ overburden pressure using a pressure gradient of 1 psi/ft. Once the specified hydrostatic and pore pressure was reached, the axial load was increased by moving the platens of the MTS load frame, between which the cell was placed, at a constant strain rate of 0.000127"/sec until the sample failed.

Variation in confining pressure in these tests was achieved by varying the pore fluid pressure while maintaining confining pressure constant.

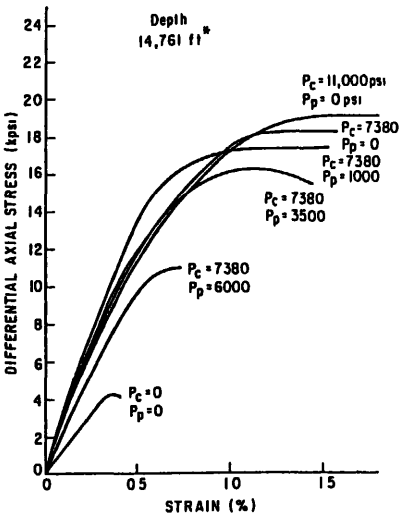

FIGURE 2 STRESS-STRAIN DIAGRAM

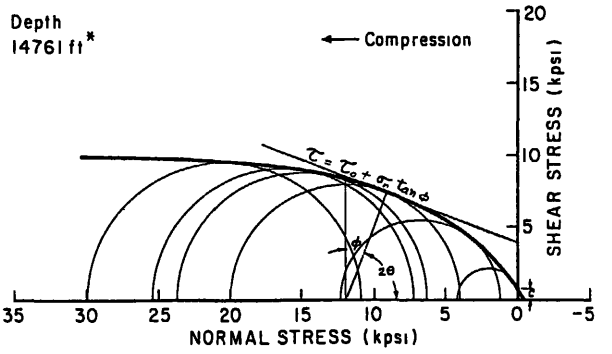

FIGURE 3 MOHR DIAGRAM

Experimental Results

A summary of triaxial tests, which includes the depths, porosity, and absolute nitrogen permeability of undeformed samples is given in Tables I.

Figs (2) and (3) respectively show typical differential axial stress versus strain curves for the samples tested and the Mohr envelope for the samples using information on their ultimate strengths.

Figs (4) and (5) show a plot of variation of ultimate strength of the rocks throughout the range of effective confining pressures for the two wells and Fig (6) and (7) show this variation with respect to pore fluid pressure. These plots show that (a) as effective confining pressure was increased, the ultimate strength, strain at failure and the angle of fracture also increased, (b) Mode of failure changed from brittle to ductile around an effective confining

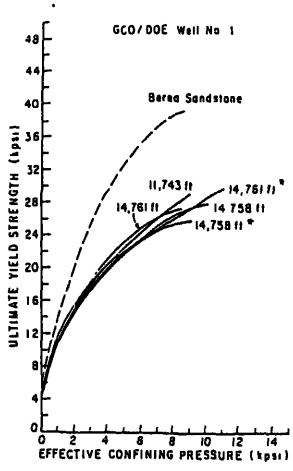

FIGURE 4

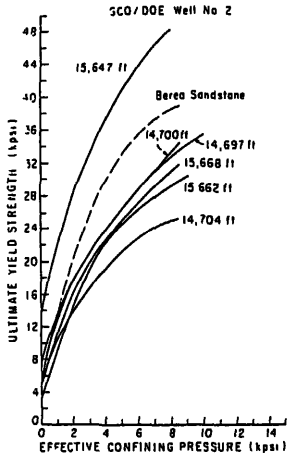

FIGURE 5

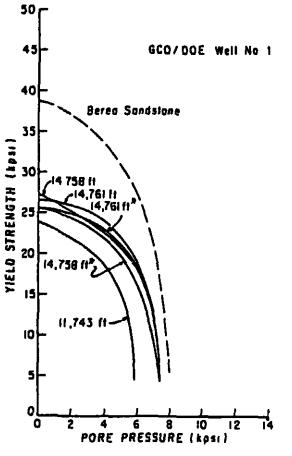

FIGURE 6

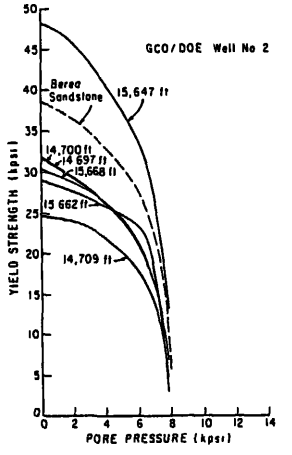

FIGURE 7

pressure of 7000 psi. For low effective confining pressures (3000 psi or less) the samples failed by brittle fracture. Fig (8) shows such a transition; the extension or shear failure is suppressed and flow becomes dominant as confining pressure increases.

It may be noted that for nearly the same porosity, (all samples from well #1 and some from well #2), the uniaxial compression strength of the samples varied from 4200 to 4600 psi. For high effective confining pressures (around 8000 psi) the strengths varied from 25000 to 27000 psi. These strengths appear to be approximately 2/3 of the corresponding values for well consolidated Berea sandstone samples tested under similar conditions.

Not all samples reached a ductile stage for the effective confining pressures used in these tests but most of them exhibited a partial ductile behavior around 5000 psi and a transition to ductile around 7000 psi.

Figures (6) and (7) show that a decrease in pore fluid pressure from the condition when both confining and pore pressure are the same, results in an increase in ultimate strength. It should, however, be noticed that an initial decrease in pore pressure by about 1000 psi increases the ultimate strength by approximately 50% compared to Berea sandstone where an increase of only 38% was observed.

A good correlation between measured and calculated values of fracture angles was observed in these samples. Computed values of fracture angles under uniaxial compression conditions varied from 12^0 to 22^0. So long as effective confining pressures were below 3000 psi, the fracture was brittle;measured and computed fracture angles matched well. Berea sandstone samples on the other hand, showed brittle fracture in this pressure range. Fracture angles increased with increasing effective confining pressure but never exceeded 43^0. The pattern of increasing fracture angles was also predicted by the Mohr Envelopes which were non-linear (Fig 3). Since most samples exhibited partial ductile behavior above 5000 psi, an accurate measurement of the fracture angles was difficult in many cases.

Figure (9) shows a typical plot of measured and calculated values of fracture angles with effective confining pressure. For most samples the curve is nonlinear as compared to Berea sandstone, Fig (10), which showed a nearly linear curve.

In well #2, a wider spectrum of uniaxial compression strengths was observed (varied from 3000 psi to 7000 psi). This was because of a wide variation in porosity of the samples. Rocks with lower porosities showed higher strengths. Effect of anisotropy was not very much pronounced. Shale samples showed brittle behavior in the range of the confining pressures used in these tests.

Conclusions

The ultimate strength and strain at failure like all other rocks increased as the effective confining pressure increased. In general, however, rocks from geopressured reservoirs appear considerably weaker than the corresponding well compacted sandstone samples. This could be attributed to under-compaction of such reservoirs and the presence of microporosity and secondary porosity.

Partial ductile behavior was observed above 5000 psi and complete transition was observed above 7000 psi in many cases. So long as effective confining pressure was less then 3000 psi, the rocks failed by brittle fracture.

Effect of pore pressure on rock strength was very much pronounced. Close correspondence between observed and calculated angles of fracture based on Mohr-Coulomb friction hypothesis suggests importance of friction.

P. N. Jogi, B. C. Llewellyn, K. E. Gray

Acknowledgements

The authors wish to express their appreciation to the technical staff of the Center for Earth Sciences and Engineering for their assistance during the experimental phase of this investigation. This work was financially supported by the U. S. Department of Energy, Geothermal Division. Their support is gratefully acknowledged.

References

1. Jones, P. H., "Geothermal Resources of Northern Gulf of Mexico," Geothermics, Special Issue 2, Vol. 2, Pt 1, 1970, pp 14-26.

2. Loucks, R. G., Richman, D. L., Milliken, K. L., "Factors Controlling Porosity & Permeability in Geopressured Frio Sandstone Reservoirs, General Crude Oil/Dept. of Energy Pleasant Bayou Test Wells, Brazoria County, Texas," Proc. 4th U. S. Gulf Coast Geopressure-Geothermal Energy Conf., Res. & Dev., Vol. 1 1979, pp 40.

3. Handin, J., Hager, R. V., Jr., "Deformation of Sedimentary Rocks under Confining Pressure," Bull. of Am. Assoc. Petr. Geol., Vol. 41, #1, Jan., 1957, pp 1-50.

4. Handin, J., Hager, R. V., Jr., Friedman, M., Feather, J. N., "Experimental Deformation of Sedimentary Rocks under Confining Pressure Pore Pressure Tests," Bull. of Am. Assoc. of Petr. Geol., Vol. 47, #5, May, 1963, pp 717-755.

5. Robinson, L. H., "Effects of Pore & Confining Pressure on Failure Characteristics of Sedimentary Rocks," Petr. Trans. AIME, Vol. 216, 1959, pp 26-32.

6. Aldrich, M. J., Jr., "Pore Pressure Effects on Berea Sandstone Subjected to Experimental Deformation," Bull. of Geol. Soc. of Am., Vol. 80, #8, 1969, pp 1577-1586.

7. Serdingecti, S. & Boozer, G. D., "The Effect of Strain Rate and Temperature on Behavior of Rocks Subjected to Triaxial Compression," Proc. of 4th Symp. on Rock Mech., Penn State, 1961, pp 83.

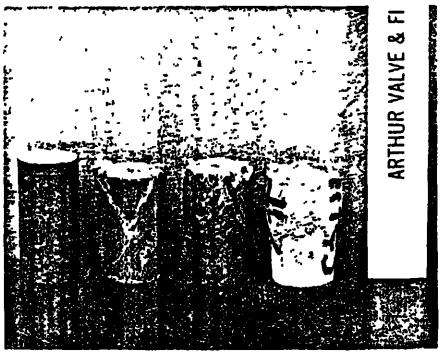

FIGURE 8

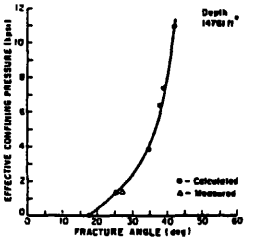

Figure 9

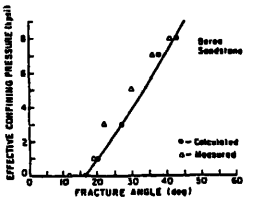

Figure 10

TABLE 1

STRENGTH CHARACTERISTICS OF GEOTHERMAL ROCKS

Sample Depth (ft.)	Absolute Permeability (md.)	Porosity (%)	Effective Confining Pressure (psi)	At Failure: Maximum Differential Axial Stress (psi)	At Failure: Effective Axial Stress (psi)	At Failure: Differential Axial Strain (%)	Young's Modulus (x10 psi)	Calculated Fracture Angle (θ_c)	Measured Fracture Angles (θ_m)	Coefficient of Internal Friction (μ)	Cohesion C (psi)
GCO-DOE #1											
11743	6.42	19.96	9000	20329	29329	1.6	2.14	39.5	--	.19	750
			5870	18041	23911	1.2	1.92	36.0	--	.32	
			4870	17286	22156	1.3	1.88	34.5	30	.38	
			2870	14624	17494	1.2	1.69	29.5	37	.60	
			870	9250	10120	0.98	1.12	25.0	25	.84	
			0	4408	4408	0.76	0.63	17.0	--	1.48	
14758	185.9	19.98	9000	18260	27260	1.06	2.85	41.5	--	.12	950
			5380	17080	22460	0.98	3.13	38.0	--	.25	
			3380	15070	18450	0.81	3.13	33.5	42	.42	
			1380	10070	12080	0.71	2.30	24.0	40	.90	
			0	4630	4630	0.53	0.60	19.5	18	1.23	
14758*	-----	19.98	7380	18230	25610	1.30	2.75	38.5	--	.23	1000
			4880	16410	21290	0.99	2.75	36.0	--	.32	
			2380	12320	14700	0.81	2.28	27.5	25	.70	
			0	4510	4510	0.45	0.78	22.0	10	1.04	
14761	124.	20.86	7380	19098	26478	1.2	3.03	41.5	--	.12	500
			5380	18548	23928	1.21	2.87	35.0	--	.36	
			3380	14997	18377	0.95	2.75	31.0	40	.53	
			1380	11808	13188	0.75	2.23	26.5	20	.75	
			0	4381	4381	0.36	1.28	16.0	--	1.60	
14761*	508.5	20.86	11000	19022	30022	1.54	2.57	42.0	--	.11	650
			7380	18159	25539	1.16	2.67	39.0	--	.21	
			6380	17287	23667	1.10	2.97	38.0	--	.25	
			3880	16238	20118	1.10	2.77	34.5	--	.38	
			1380	11001	12381	0.73	2.17	25.5	27	.81	
			0	4218	4218	0.36	1.3	17.5	--	1.43	
GCO-DOE #2											
14697	7.58	16.29	10,000	25,460	35,460	1.21	4.12	38.5	--	.23	1,100
			5,350	21,900	27,250	0.85	3.92	35.0	43	.36	
			3,350	18,740	22,090	0.73	3.68	30.0	--	.58	
			1,350	13,940	15,290	0.77	2.88	26.0	28	.78	
			0	7,024	7,024	0.43	1.72	17.5	--	1.43	
GCO-DOE #2											
14700	---	16.21	7,350	24,583	31,933	1.10	3.5	40.0	35	.18	800
			6,350	23,406	29,756	0.95	3.5	31.5	25	.51	
			4,350	19,548	23,898	0.75	3.5	30.5	35	.55	
			2,350	16,613	18,963	0.74	3.5	28.0	25	.67	
			350	8,350	8,700	0.49	2.2	21.0	23	1.11	
			0	4,538	4,538	0.44	1.15	15.5	26	1.66	
14709	357.	20.9	7,350	17,250	24,600	1.08	2.99	42.0	--	.11	850
			5,350	16,660	22,010	1.08	2.80	38.5	--	.23	
			3,350	14,280	17,630	1.02	2.70	33.0	--	.45	
			1,350	10,600	11,950	0.71	2.35	27.5	--	.70	
			0	4,845	4,845	0.40	1.55	19.5	--	1.23	
15630	< 0.1 md.**		7,820	18,880	26,700	1.30	1.60	42.5	40	.09	1,200
15628			4,000	18,110	22,110	1.30	1.47	35.0	30	.36	
15628			1,000	10,820	11,820	1.12	1.01	23.5	22	.93	
15671			7,835	17,960	25,795	1.22	----	----	--	----	
15647	0.197	10.72	7,825	40,460	48,285	1.17	5.50	37.0	--	.29	2,000
			5,825	37,990	43,815	1.09	5.28	30.0	--	.58	
			3,825	32,920	36,745	0.91	4.90	26.0	28	.78	
			1,825	25,620	27,445	0.75	4.15	23.0	25	.97	
			0	13,400	13,400	0.51	2.60	17.0	--	1.48	
15662	----	----	7,830	21,190	29,020	1.04	4.23	38.0	--	.25	500
			5,830	19,700	25,530	0.99	3.53	36.5	--	.31	
			3,830	17,950	21,780	0.90	3.50	34.5	--	.38	
			1,830	15,420	17,250	0.89	3.00	31.0	37	.53	
			0	3,170	3,170	0.39	0.90	12.0	--	2.25	
15668	38	18.29	7,830	22,680	30,510	1.08	3.60	39.0	--	.21	750
			4,830	19,805	24,635	0.93	3.60	33.0	--	.45	
			1,830	13,660	15,490	0.93	2.62	26.0	--	.78	
			0	4,758	4,758	0.35	1.45	16.5	--	1.54	
Berea Sample	201.8	20.17	8,000	30,670	38,670	1.39	3.00	43.0	41	.07	1,200
			7,000	30,390	37,390	1.30	3.28	38.0	36	.25	
			5,000	27,060	32,060	1.39	3.00	30.0	30	.36	
			3,000	22,630	25,630	1.27	2.72	27.0	22	.93	
			1,000	13,040	14,040	0.86	1.98	20.0	19	1.19	
			0	5,785	5,785	0.67	0.90	16.5	12	1.54	

* Specimen cut perpendicular to the core

** Shale Samples